Aalborg Universitet

Gas diffusion characteristics of agricultural soils from South Greenland

Weber, Peter L.; de Jonge, Lis Wollesen; Greve, Mogens H.; Norgaard, Trine; Moldrup, Per

SOIL PHYSICS & HYDROLOGY

Gas diffusion characteristics of agricultural soils from South Greenland

Peter L. Weber[1] ⓘ | **Lis Wollesen de Jonge[1]** | **Mogens H. Greve[1]** | **Trine Norgaard[1]** | **Per Moldrup[2]**

[1] Dept. of Agroecology, Faculty of Technical Sciences, Aarhus Univ., Blichers Allé 20, 4 P.O. Box 50, Tjele DK-8830 Denmark

[2] Dept. of the Built Environment, Aalborg Univ., Thomas Manns Vej 23, Aalborg Ø DK-9220 Denmark

Correspondence
Dept. of Agroecology, Faculty of Sciences and Technology, Aarhus University, Blichers Allé 20, 4 P.O. Box 50, DK-8830 Tjele, Denmark.
Email: plw@agro.au.dk

Funding information
Teknologi og Produktion, Det Frie Forskningsråd, Grant/Award Number: 8022-00184B

Abstract

The Arctic is warming at twice the global average, which may impact agricultural production in Greenland. Therefore knowledge of the functional properties of Greenlandic soil resources is necessary. The relative soil gas diffusivity [the soil gas diffusion coefficient (D_p)–free-air diffusion coefficient (D_o) ratio] is the chief parameter controlling gas transport in soils. Predictions of D_p/D_o are needed to estimate root zone aeration and terrestrial greenhouse gas fluxes. We used existing models to analyze the D_p/D_o of soils from Greenlandic fields and a pore connectivity index (C_{ip}) to infer their degree of structural development and identify the main parameters controlling D_p/D_o. In total, 201 × 3 intact 100-cm^3 soil samples were sampled across six fields with clay and organic C contents of 0.016 to 0.089 and 0.016 to 0.105 kg kg^{-1}, respectively. The D_p/D_o was measured with the one-chamber nonsteady-state method at soil water potentials between –10 and –1,000 cm H_2O. Accurate determination of total porosity (Φ) was ensured by calibrating a particle density model on 129 samples. The soils exhibited a less developed structure and highly tortuous pore networks, resulting in low D_p/D_o as a function of air-filled porosity (ε). Density-corrected models with air saturation (ε/Φ) reduced the RMSE. Furthermore, C_{ip} at –1,000 cm H_2O soil water potential increased linearly with dry bulk density (ρ_b), suggesting that ρ_b is a key controller of D_p/D_o, which is important for planning cultivation practices for Southern Greenlandic soils. Lastly, we found that an air saturation >35% is required for adequate soil aeration.

Abbreviations: CF, coarse fraction; C_{ip}, pore connectivity index; D_o, diffusion coefficient of oxygen in free air; D_p, oxygen soil gas diffusion coefficient; D_p/D_o, relative soil gas diffusivity; GDC, generalized density-corrected model; GHG, greenhouse gas; IG-1, Igaliku Site 1; IG-2, Igaliku Site 2; OC, organic C; MPD, macroporosity-dependent model; MQ(61), Millington and Quirk (1961) model; SI-1, South Igaliku Site 1; Si-2, South Igaliku Site 2; SI-3, South Igaliku Site 3; SOM, soil organic matter; UP, Upernaviasuk; ε, air-filled porosity; ρ_b, dry bulk density; ρ_s, particle density; Φ, total porosity.

1 | INTRODUCTION

Because of anthropogenic and natural GHG emissions, climate change is currently transforming the Arctic region at an alarming rate. The region is warming approximately twice as fast as the global average (Francis & Vavrus, 2012), which has severe repercussions for the Arctic ecosystems and, consequently, the food security and livelihoods of the indigenous Arctic peoples (Nuttall, 2018). The warmer

climate can, however, offer better conditions for future agricultural production in southwest Greenland because of the increased summer temperatures, which are projected to prolong the growing season by ~2 mo by 2100 (Caviezel, Hunziker, & Kuhn, 2017; Christensen, Olesen, Boberg, Stendel, & Koldtoft, 2016; Westergaard-Nielsen et al., 2015). Nevertheless, successful agriculture is contingent on more than climatic factors. The soil's physical functional properties (e.g., their ability to facilitate gas exchange) are paramount for sustaining agricultural production (Doran & Parkin, 1994). Additionally, accurate predictions of gas exchange within the soil and across the soil–atmosphere boundary are critical for evaluating the terrestrial fluxes of GHGs such as CO_2, N_2O, and CH_4 (Schulze et al., 2009; Smith et al., 2000).

The soil resource is arguably the biggest unknown factor for the agricultural production in southwest Greenland and the majority of the soil-related research has been of an archeological and paleogeographical nature (Adderley & Simpson, 2006; Massa et al., 2012; Rutherford, 1995; Schofield et al., 2010), with only a few studies having investigated some basic physical properties of the soils. In general, the soils have been found to exhibit little to moderate soil formation (Jacobsen, 1987; Jakobsen, 1991; Rutherford, 1995), while being shallow, highly acidic, organic, and coarse-textured with a noteworthy low clay content (Adderley & Simpson, 2006; Caviezel et al., 2017; Ogrič et al., 2019). On the basis of a combination of chemical soil properties, texture, and ρ_b, Caviezel et al. (2017) evaluated the soil quality to be relatively poor in part of the agricultural area. Up until now, the functional properties of the Greenlandic soil resource remain largely undescribed and no studies have investigated the gas phase transport properties of Greenlandic soils outside the permafrost-affected high Arctic peatlands.

The ability of soil to facilitate oxygen diffusion is governed by the oxygen soil gas diffusion coefficient, D_p (m^3 m^{-1} s^{-1}), which is typically normalized with the diffusion coefficient of oxygen in free air (D_o) and expressed as the D_p/D_o. This normalization isolates the effects of soil pore characteristics by eliminating the effect of temperature, pressure, and gas-specific characteristics. Within the vadose zone, the exchange of gases primarily occurs via diffusion through the gaseous phase (Penman, 1940). Consequently, D_p/D_o has been intimately linked with, for example, soil aeration (Ball, 2013; Stepniewski, 1981), N_2O and N_2 emissions (Deepagoda, Clough, Thomas, Balaine, & Elberling, 2019; Petersen, Schjønning, Thomsen, & Christensen, 2008), production and oxidation of CH_4 (Smith et al., 2000), and CO_2 emissions from microbial respiration (Tang & Riley, 2019).

Measuring D_p/D_o is instrumentally complex and time-consuming. Several empirical and semi-physical models

Core Ideas

- Soil gas diffusivity (D_p/D_o) was measured on Greenlandic agricultural soil samples.
- Data were analyzed with existing D_p/D_o models and a pore connectivity index (C_{ip}).
- Density-corrected D_p/D_o models performed better than other model types.
- The C_{ip} indicated a less developed soil structure with tortuous pore networks.
- Air saturation of >35% is probably needed for adequate soil aeration ($D_p/D_o > 0.02$).

have therefore been developed for predicting D_p/D_o from the soil's physical parameters such as ε, Φ, texture, and pore size distribution (Buckingham, 1904; Deepagoda et al., 2011a; Millington & Quirk, 1960, 1961; Moldrup, Olesen, Schjønning, Yamaguchi, & Rolston, 2000; Resurreccion et al., 2010). Because of these models' empirical nature, no single model has proved universally applicable and the performance of the individual models remains highly dependent on soil type (Deepagoda, de Jonge, Kawamoto, Komatsu, & Moldrup, 2015; Iiyama & Hasegawa, 2005; Jin & Jury, 1996). Furthermore, the application of these models remains uncertain for subarctic agricultural soils, as the D_p/D_o characteristics of these soils are still completely undescribed.

By definition, D_p/D_o is governed by the volume, tortuosity, and connectivity of the air-filled pore space and thus provides valuable information about the soil structure (Moldrup, Olesen, Komatsu, Schjønning, & Rolston, 2001). A number of structural indices have therefore been proposed in the literature to infer the soil's structural architecture from D_p/D_o (Ball, 1981; Deepagoda et al., 2015; Moldrup et al., 2001).

The air-filled pore space is the principal pathway of soil gas diffusion and thus D_p/D_o is intimately related to ε (Buckingham, 1904). Notwithstanding the water content, precise determination of ε hinges on an accurate determination of the ρ_b and the particle density (ρ_s); special attention therefore needs to be given to ρ_b and ρ_s when evaluating the D_p/D_o characteristics, especially in soils as undescribed as those in Greenland.

This study provides the first comprehensive investigation of the D_p/D_o characteristics of Greenlandic agricultural soils based on measurements of 201 intact and variably saturated topsoil samples originating from six Greenlandic fields. We hypothesized that the unique climatic and pedological nature of the Greenlandic soils would result in markedly different D_p/D_o characteristics compared with temperate agricultural soils. To test this
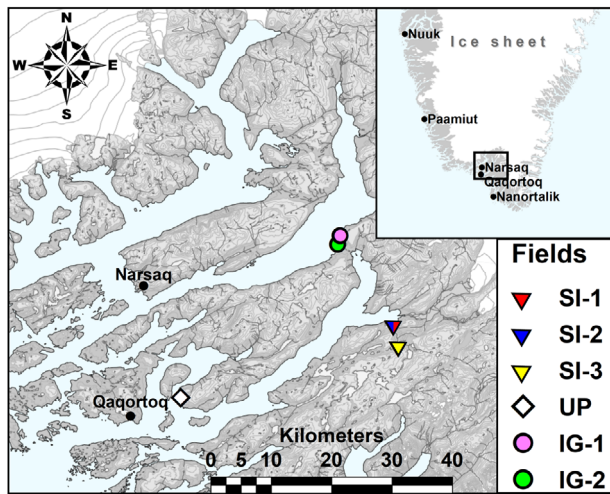
FIGURE 1 Location of the six agricultural field sites, which are situated in the Tunulliarfik and Igalikup Kangerlua fjord systems. The fields are located across the three areas of South Igaliku (SI), Upernaviasuk (UP), and Igaliku (IG)

hypothesis, the primary objectives were to: (a) analyze the D_p/D_o characteristics by comparing the Greenlandic soils with temperate soils via the D_p/D_o models available in the literature, (b) evaluate the applicability of existing D_p/D_o models on the Greenlandic soils, (c) use a recently proposed soil pore connectivity index, C_{ip}, to both infer the soil structure and identify the main physical parameters governing D_p/D_o in Greenlandic agricultural soils. A further objective was to ensure accurate predictions of ε and Φ by evaluating the ρ_s–OC relationships in the Greenlandic soils.

2 | MATERIALS AND METHODS

2.1 | Study area

The six studied fields are located within three areas: South Igaliku (SI-1 and SI-2, 60°53′29.2″N, 45°16′27.8″W; SI-3, 60°51′39.1″N, 45°16′26.4″W), Upernaviasuk (UP, 60°45′22.7″N, 45°53′36.5″W), and Igaliku (IG-1, 61°01′08.9″N, 45°27′39.4″W; IG-2, 61°00′22.7″N, 45°27′57.7″W). All three areas lie within the main agricultural area in southwest Greenland along the marginal ice-free border between the Greenland ice sheet and the Davis Strait (Figure 1). Agriculture has a rich history in the area and was first practiced during the Norse Landnám (c.a. 985–1450 AD), which coincided with the Medieval climate anomaly (Bichet et al., 2013; Dugmore, Keller, & McGovern, 2007). Modern sheep farming was introduced in 1982 after ~200 yr of small-scale subsistence farming (Jacobsen, 1987). The three areas lie within the

boundaries of the newly designated Kujataa UNESCO world heritage site, ratifying the beauty and cultural importance of the agricultural landscape.

The climate varies considerably within the study area because of the local topography and the distance from the ocean (Christensen et al., 2016). The climate changes from oceanic in the outer parts of the fjords (UP) through to suboceanic (SI-1, SI-2, and SI-3) to subcontinental in the inner fjords (IG-1 and IG-2) (Jacobsen, 1987). The mean annual temperature and precipitation range from 0.9 °C and 615.1 mm in the inner fjords to 0.6 °C and 857.6 mm in the outer fjords (Hanna & Cappelen, 2002). The study area is situated south of the discontinuous permafrost zone (Daanen et al., 2011) and the cultivated fields in the area are not affected by permafrost.

All six fields had a cropping history of perennial grass mixtures for either winter fodder production (SI-3, UP, IG-1, and IG-2) or pasture (SI-1 and SI-2). The vegetation at the time of sampling was perennial grass mixtures, with the exception of oat (*Avena sativa* L.) on UP. The grass mixtures typically consisted of a combination of timothy (*Phleum pratense* L.), colonial bentgrass (*Agrostis tenuis* L.), Kentucky bluegrass (*Poa pratensis* L.), and red fescue (*Festuca rubra* L.). The SI-1 and SI-2 sites had no recent history of tillage, whereas UP and IG-1 were tilled in the spring prior to sampling and SI-3 and IG-2 had not been tilled within the last 3 yr.

2.2 | Soil sampling

A total of 201 field points were sampled across the six fields in August 2013, 2015, and 2017, with rectangular grids at 7.5- by 7.5-m spacing for SI-2, and 15- by 15-m spacing for the remaining five fields. In each field point, undisturbed soil samples were collected in triplicate with 100-cm³ steel cores. Bulk soil was sampled between the cores for characterization of bulk soil properties. All field points were sampled in the A-horizon immediately below the thatch layer at a depth of ~10 to 15 cm. The cores were stored at 2 °C until analysis and the bulk soil was air-dried, crushed, and subsequently passed through a 2-mm sieve.

2.3 | Bulk soil samples

Soil texture was determined by a combination of wet sieving and the pipette or hydrometer methods (Gee & Or, 2002) after the removal of soil organic matter (SOM). The soil OC was measured with a LECO C analyzer (LECO Corporation, St Joseph, MI) coupled to a CO_2 detector (Thermo Fisher Scientific Inc., Waltham, MA). The SOM was inferred via a conversion factor of 0.58 (Pribyl, 2010).

The ρ_s was determined on a subset of 129 bulk soil samples by the pycnometer method (Blake & Hartge, 1986). The subset consisted of all 58 soils from the IG fields and 17, 11, 12, and 31 samples from SI-1, SI-2, SI-3, and UP, respectively. The ρ_s values of the remaining 72 soils were estimated by calibrating the following organic- and mineral-dependent ρ_s model proposed by Rühlmann, Körschens, and Graefe (2006) on the 129 measured samples:

$$\rho_s = \left(\frac{OM_f}{\rho_{om}} + \frac{(1 - OM_f)}{\rho_{ms}} \right)^{-1}, \quad (1)$$

where OM_f is the gravimetric SOM fraction (kg kg^{-1}), ρ_{om} is the density of the gravimetric SOM fraction (Mg m^{-3}), and ρ_{ms} is the density of the mineral fraction (Mg m^{-3}).

2.4 | Undisturbed soil cores

The undisturbed soil cores were saturated and subsequently drained stepwise up to seven soil water matric potentials (ψ) between pF1 and pF3, where pF = log[ψ, in cm H$_2$O], following Schofield (1935), a combination of tension tables and Richards' pressure plate apparatuses (high flow pressure plate cells, 0675B01M3, Soilmoisture Equipment Corp., Santa Barbara, CA). The range and number of measured matric potentials at which the measurements were done varied between the fields, with the highest soil water matric potential being pF1 for SI-1, SI-2, SI-3, and UP; pF1.48 for IG-1; and pF1.7 for IG-2. The lowest soil water matric potential was pF2 for UP and pF3 for the remaining five fields, which resulted in 3336 retention points across the 201 × 3 soil cores.

At each drainage step, D_p/D_o was determined via the one-chamber non-steady-state method (Rolston & Moldrup, 2002), with the same experimental setup and procedure described by Schjønning, Eden, Moldrup, and de Jonge (2013a). Briefly, one side of the soil core was put into contact with a reservoir chamber, which was initially purged with N$_2$ at the start of the measurement. The increase in O$_2$ concentration caused by the diffusive flux was subsequently determined every 2 min by an oxygen sensor (Figaro KE-12, Figaro Engineering Inc., Osaka, Japan), which was mounted inside the reservoir chamber. The measurements were taken in a climate-controlled laboratory at 20 °C for 0.5 to 2 h, depending on the D_p/D_o of the samples. A value of 0.205 cm^2 s^{-1} was used for D_o at 20 °C at 1.013 × 10^5 Pa (Schjønning et al., 2013a).

The soil cores were weighed at each drainage step and ρ_b was determined after oven-drying the soil cores for 48 h at 105 °C. The gravimetric coarse fraction (CF) content (>2 mm) was determined by passing the oven-dried soil cores through a 2-mm sieve. Lastly, the volumetric water content, the ε, and the air saturation at each drainage step were determined from the core-specific ρ_s. The core-specific ρ_s were obtained by correcting the 129 measured and 72 estimated ρ_s values for the CF (assuming a CF density of 2.65 Mg m^{-3}).

2.5 | Soil gas diffusivity models

In his seminal work, Buckingham (1904) suggested the use of a simple power-law function to predict D_p/D_o from ε:

$$\frac{D_p}{D_o} = \varepsilon^X. \quad (2)$$

On the basis of his measurements on relatively dry porous media, he suggested setting the exponent $X = 2$ but other authors have suggested setting $X = 1.5$ (Marshall, 1959) and $X = 1.33$ (Millington, 1959). Buckingham's exponent X has subsequently been applied as a structural fingerprint to infer the tortuosity of the air-filled soil pores (Currie, 1960; Deepagoda et al., 2012; Schjønning et al., 2013b).

A generalized version of the macroporosity-dependent model (MPD) developed by Moldrup et al. (2000) was used to compare the D_p/D_o–ε characteristics of the Greenlandic soils with temperate Danish soils:

$$\frac{D_p}{D_o} = 2\varepsilon^3 + 0.04\varepsilon. \quad (3)$$

The MPD model was originally used to successfully model ($r^2 = 0.97$) the D_p/D_o of 126 cultivated Danish soils at pF2 based on ε at pF2. Subsequently, Deepagoda et al. (2011b) proposed the generalized MPD in Equation (3) and found it to represent 30 Danish soils of mixed origin across a larger range in soil water matric potentials.

To evaluate the applicability of existing D_p/D_o models on the Greenlandic soils, this study compared the descriptive–predictive performance of a Buckingham-type power model (Equation 2), and the widely used empirical model developed by Millington and Quirk (1961) [MQ(61) model]:

$$\frac{D_p}{D_o} = \frac{\varepsilon^{10/3}}{\Phi^2}, \quad (4)$$

where Φ denotes the total porosity (m^3 m^{-3}) of the soil sample.

In addition, this study evaluated the unimodal generalized density-corrected (GDC) model proposed by Deepagoda et al. (2011a):

$$\frac{D_p}{D_o} = \alpha \left(\frac{\varepsilon}{\Phi} \right)^{\beta}, \tag{5}$$

where α and β are numerical shape parameters that represent the connectivity and tortuosity of the functional air-filled pore network, respectively.

The GDC model was inspired by the observations of Deepagoda et al. (2011b), who found a marked reduction in density-induced fluctuations when D_p/D_o was expressed as a function of air saturation (ε/Φ) rather than ε. Subsequently, Deepagoda et al. (2011a) found a linear relationship between the shape parameters and Φ and proposed $\alpha = 0.5\Phi$ and $\beta = 2 + 1.38\Phi$, derived from a wide range of data on both repacked and weakly structured intact soil samples from the literature.

2.6 | Structural fingerprinting

In order to identify the main physical parameters governing the D_p/D_o of the investigated soils, we applied the C_{ip}, which was recently proposed by Deepagoda et al. (2015):

$$C_{ip} = \frac{\log(\varepsilon)}{\log\left(\frac{D_p}{D_o}\right)}. \tag{6}$$

The C_{ip}–ε characteristic has successfully been applied to track the differences in soil structure caused by compaction and hierarchal soil structures (e.g., aggregates and fractures) (Deepagoda et al., 2015). The index ranges from 0 to 1, representing the range from a complete absence of connected air-filled pores to a fully connected and straight air-filled pore network. It should be noted that C_{ip} is the reciprocal of Buckingham's X in Equation (2). Because of the inherent uncertainty of index at low ε values, we applied a cutoff value of 0.02 m^3 m^{-3}. In order to perform a comparison between the C_{ip}–ε/Φ characteristics of the Greenlandic soils and temperate Danish soils, the generalized MPD model Equation (2) was substituted into Equation (6), yielding:

$$C_{ip:MPD} = \frac{\log(\varepsilon)}{\log(2\varepsilon^3 + 0.04\varepsilon)}, \tag{7}$$

where $C_{ip:MPD}$ denotes the C_{ip} derived from the MPD model at a given ε.

2.7 | Statistical analysis

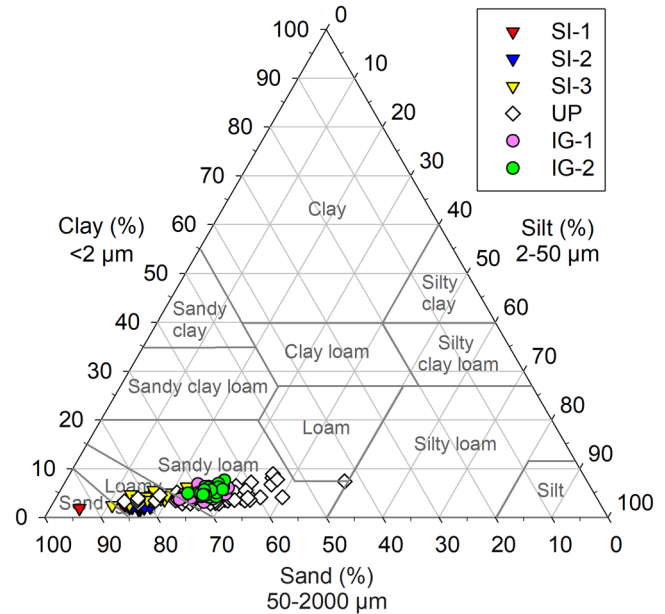The RMSE was used for fitting the models in Microsoft Excel (Microsoft Corp., Redmond, WA) via the GRG Non-

FIGURE 2 Distribution of the 201 soil samples in the USDA soil textural classes. SI, South Igaliku; UP, Upernaviasuk; IG, Igaliku

linear algorithm. Both RMSE and bias were used to evaluate and compare the descriptive–predictive performance of the D_p/D_o models investigated. The RMSE indicates how well the model fits with the measured data:

$$RMSE = \sqrt{\frac{1}{n} \sum_{i=1}^{n} (d_i)^2}, \tag{9}$$

where d_i is the difference between the predicted and measured values for the number of measurements (n). The bias indicates the overall level of bias in the prediction; in other words, if the model in question results in a general overprediction (positive bias) or underprediction (negative bias):

$$bias = \frac{1}{n} \sum_{i=1}^{n} (d_i). \tag{10}$$

3 | RESULTS AND DISCUSSION

3.1 | Soil texture and OC

The soils investigated in this study were predominately coarse-textured and occupied the USDA textural classes of sand to sandy loam (Figure 2). The clay content ranged between 0.016 and 0.089 kg kg^{-1} across all fields (Table 1). The SI-1 and SI-2 soils had the lowest mean clay content at 0.029 and 0.022 kg kg^{-1}, which was slightly lower than in the soils from SI-3, UP, IG-1, and IG-2 at 0.040, 0.044, 0.044, and 0.049 kg kg^{-1}, respectively. The mean silt content was

**TABLE 1**　Selected soil physical properties across the investigated fields[a]

Field	Value	Organic C	Clay content	Silt content	Particle density[b]	Bulk density	Total porosity[c]	Coarse fraction[d]
		kg kg⁻¹			Mg m⁻³		m³ m⁻³	kg kg⁻¹
SI-1 (n = 32)	Mean	0.039	0.029	0.035	2.63	1.12	0.58	–
	Min.	0.016	0.018	0.017	2.56	0.92	0.50	–
	Max.	0.081	0.045	0.047	2.68	1.35	0.65	–
	σ	0.013	0.006	0.006	0.03	0.12	0.04	–
SI-2 (n = 18)	Mean	0.026	0.022	0.032	2.68	1.28	0.52	–
	Min.	0.018	0.016	0.017	2.65	1.19	0.49	–
	Max.	0.037	0.029	0.036	2.70	1.37	0.55	–
	σ	0.005	0.004	0.005	0.01	0.05	0.02	–
SI-3 (n = 24)	Mean	0.059	0.040	0.044	2.61	1.08	0.58	–
	Min.	0.022	0.024	0.020	2.57	0.80	0.48	–
	Max.	0.105	0.056	0.087	2.66	1.38	0.68	–
	σ	0.019	0.008	0.014	0.03	0.15	0.05	–
UP (n = 69)	Mean	0.041	0.044	0.106	2.55	1.21	0.53	0.322
	Min.	0.020	0.028	0.063	2.36	0.86	0.45	0.091
	Max.	0.079	0.089	0.305	2.65	1.46	0.64	0.689
	σ	0.012	0.014	0.045	0.05	0.13	0.05	0.110
IG-1 (n = 28)	Mean	0.066	0.044	0.087	2.47	0.91	0.64	0.028
	Min.	0.045	0.028	0.073	2.38	0.74	0.55	0.001
	Max.	0.097	0.059	0.098	2.55	1.24	0.70	0.167
	σ	0.011	0.008	0.007	0.04	0.10	0.04	0.034
IG-2 (n = 30)	Mean	0.059	0.049	0.091	2.49	0.96	0.62	0.040
	Min.	0.041	0.037	0.076	2.44	0.85	0.56	0.004
	Max.	0.080	0.067	0.104	2.56	1.13	0.66	0.222
	σ	0.010	0.007	0.006	0.03	0.07	0.03	0.042

[a] Organic C, clay, silt, and particle density determined from bulk soil. Bulk density, total porosity and coarse fraction were determined on the soil cores.

[b] Particle density was determined on all Igaliku (IG) soils and for 17, 11, 12, and 31 samples for South Igaliku (SI) sites SI-1, SI-2, SI-3, and Upernaviasuk (UP), respectively. The remaining particle densities were predicted via Equation (1).

[c] The total porosities of the soil cores were calculated from the coarse fraction-adjusted particle densities.

[d] Coarse fraction (i.e., the content of minerals > 2 mm) of the soil cores. The coarse fraction was considered to be negligible for SI-1, SI-2, and SI-3.
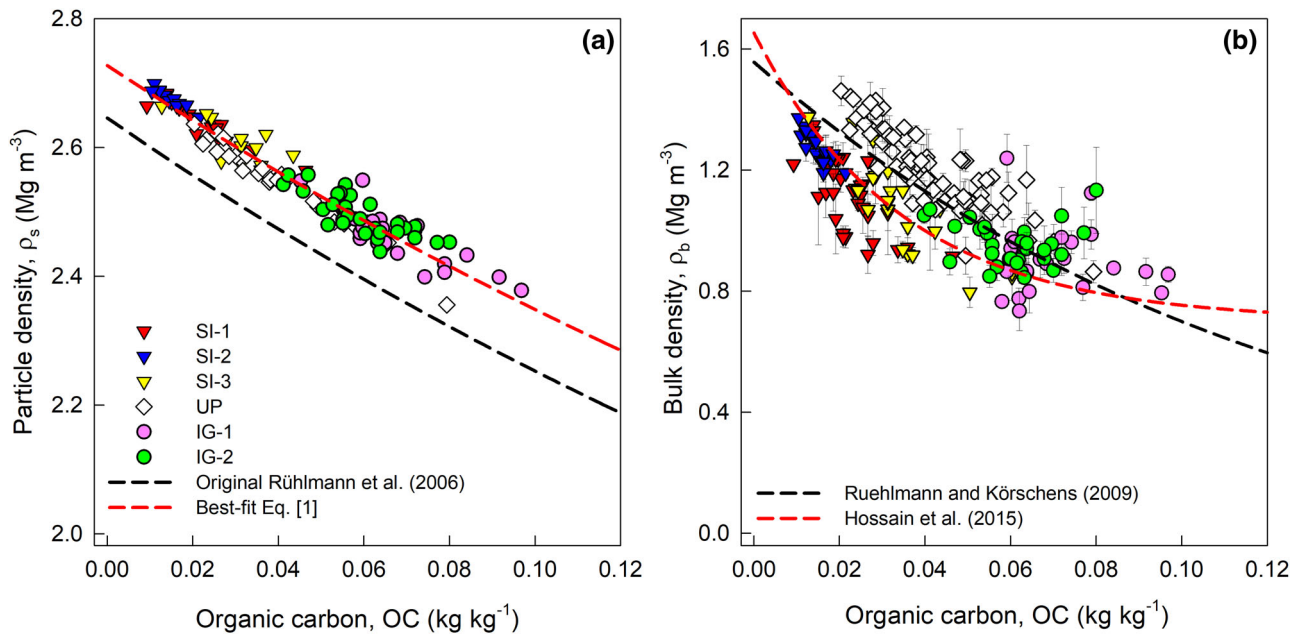
FIGURE 3 (a) Soil particle density as a function of organic C content across the six fields. The black dashed line represents the particle density model developed by Rühlmann et al. (2006) (Equation 1) on 170 soils of predominately temperate origin. The red dashed line represents the best fit of the same model on the Greenlandic soils. (b) Bulk density as a function of organic C content for all 201 samples. The black dashed line represents the particle density model developed by Ruehlmann and Körschens (2009) on 163 arable soils from northern Europe, the United States, and India. The red dashed line represents the best fitting model developed by Hossain et al. (2015) on 702 mineral Arctic and sub-Arctic soils from northwestern Canada. Error bars denote the SD. SI, South Igaliku; UP, Upernaviasuk; IG, Igaliku

notably lower for the SI fields (0.032–0.044 kg kg⁻¹) than for the UP and IG fields (0.087–0.106 kg kg⁻¹). The CF was negligible for the SI soils and ranged between 0.000 and 0.689 kg kg⁻¹ across the other five fields. It was notable that the UP soils had a significantly higher mean CF content of 0.322 kg kg⁻¹ than the IG-1 and IG-2 soils at 0.028 and 0.040 kg kg⁻¹, respectively. The OC ranged between 0.016 and 0.105 kg kg⁻¹ across all soils and was lower for SI-1, SI-2, and UP (mean: 0.026–0.041 kg kg⁻¹) than for SI-3, IG-1, and IG-2 (mean: 0.059–0.066). These textural ranges agreed well with previous studies, which reported predominately loamy sand to sandy loam soils in the IG and UP areas (Caviezel et al., 2017; Rutherford, 1995) and sand loess adjacent to SI-1 and SI-2 (Jacobsen, 1987).

3.2 | Particle density and ρ_b

The ρ_s values of Greenlandic soils were negatively correlated with OC and varied between 2.36 and 2.70 Mg m⁻³ across the fields (Table 1). Fitting Equation (1) to the measured ρ_s resulted in a good fit across all fields (Figure 3a), which implied that the average ρ_{om} and ρ_{ms} were 1.41 and 2.73 Mg m⁻³, respectively. The Greenlandic soils thus exhibited markedly higher ρ_s than those in Rühlmann et al. (2006), who reported the average ρ_{om} and ρ_{ms} to be 1.35 and 2.65 Mg m⁻³, respectively, for

170 soils of widely varying composition and origin. The high ρ_{om} is somewhat surprising, considering the low clay contents (Schjønning, McBride, Keller, & Obour, 2017) and indicates the presence of mineralogical components heavier than quartz (Rühlmann et al., 2006). Furthermore, the lower ρ_{om} reported by Rühlmann et al. (2006) was obtained with an OC–SOM conversion factor of 0.55, which increased the disparity, as this conversion factor resulted in a ρ_{om} of 1.44 for the Greenlandic soils. Further evaluation of the OC–SOM conversion factor would provide valuable insights into the nature of this Arctic SOM but is beyond the scope of the present study.

The ρ_b of the Greenlandic soils decreased with OC (Figure 3b) and ranged between 0.80 and 1.46 Mg m⁻³. The UP soils generally exhibited higher ρ_b because of their larger CF content. On the contrary, the SI soils displayed lower ρ_b despite their low OC compared with the UP soils, whereas the IG soils exhibited a larger degree of variation in the ρ_b–OC relationship. Bulk density exhibited a small but significant negative correlation with clay content ($P < .001$; $r^2 = 0.07$). The SI soils exhibited a similar ρ_b–OC trend to that reported by Hossain, Chen, and Zhang (2015) for 702 mineral Arctic and sub-Arctic soils across northwestern Canada, whereas the ρ_b of the UP and IG soils resembled the trend reported for 163 arable soils from northern Europe, the United States, and India by Ruehlmann and Körschens (2009).
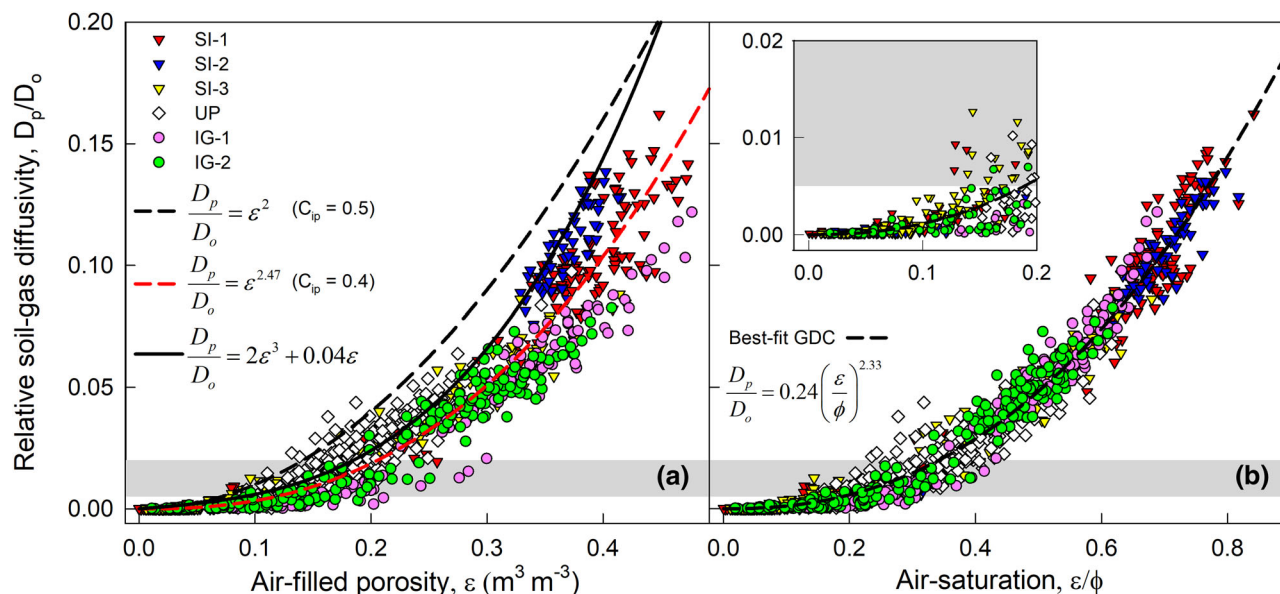
FIGURE 4 (a) Measured relative soil gas diffusivity [the soil gas diffusion coefficient (D_p)–free-air diffusion coefficient ratio, D_p/D_o] as a function of air-filled porosity (ε) for the six Greenlandic fields and the Buckingham (1904) model (black dashed lines), the best fitting Buckingham-type model (red dashed lines), and the macropore-dependent model (solid black), which represents 126 Danish soils. (b) Relative soil gas diffusivity as a function of air saturation with the best fitting generalized density-corrected (GDC) model (Equation 5) with $\alpha = 0.24$ and $\beta = 2.33$ (black dashed lines). The inserted graph depicts an enlarged part of the low D_p/D_o region in (b). The gray area represents the lower boundary for sufficient soil aeration (Schjønning et al., 2003; Stępniewski, 1981). SI, South Igaliku; UP, Upernaviasuk; IG, Igaliku

3.3 | Soil gas diffusivity

The investigated soils exhibited low and variable D_p/D_o when plotted against ε (Figure 4a). Stępniewski (1981) and Schjønning, Thomsen, Moldrup, and Christensen (2003) reported that both soil aeration and aerobic microbial activity diminished rapidly at D_p/D_o values between 0.005 and 0.02 for temperate soils of varying texture and ρ_b. Sufficient aeration is generally first exceeded at $\varepsilon > 0.2$ m^3 m^{-3} for the Greenlandic soils if the lower boundary for sufficient aeration is considered to be a D_p/D_o of 0.02. The reference Buckingham model significantly overpredicted the measured values and effectively represented a conservative upper boundary for D_p/D_o across all fields. Fitting the Buckingham-type model in Equation (2), to the measured data resulted in an exponent of 2.47, which, conversely, represents a shift in C_{ip} from 0.5 to 0.4. The MPD model, which represents measurements of 126 intact Danish cultivated soils (Moldrup et al., 2000), also resulted in an overestimation, with the exception of UP soils. The D_p/D_o was generally lower for the less dense, finer textured, and more organic IG fields than for the coarser textured and less organic SI-1 and SI-2 sites. The higher D_p/D_o in the dense soils than in the more porous soils at a given ε has also been reported for temperate soils (Deepagoda et al., 2011a; Fujikawa & Miyazaki, 2005). Fujikawa and Miyazaki (2005) attributed the effect to a preferential loss of ineffective pore space following compaction, whereas

Deepagoda et al. (2011a) attributed it to a reduced water bridging effect, as dense soils contain less water than more porous soils (and consequently higher air saturation) at a given ε.

Plotting D_p/D_o against air saturation (Figure 4b) markedly reduced the inter- and intrafield variation, which points to soil density being the major physical parameter governing the D_p/D_o of the Greenlandic soils. The reduction in density-induced effects allowed a good fit of Equation (5) with $\alpha = 0.24$ and $\beta = 2.33$, which further revealed that the lower boundary for sufficient aeration (i.e., $D_p/D_o > 0.02$) (Schjønning et al., 2003; Stepniewski, 1980, 1981) was generally exceeded at air saturation levels above 0.35. The high degree of air saturation needed for sufficient aeration still highlights the risk of hypoxia, especially on poorly drained fields such as SI-3, which displayed a mean actual air saturation of 0.16 at the time of sampling, despite 2015 being a relatively dry growing season. In contrast, the nearby SI-1 and SI-2 soils displayed a mean air saturation of 0.77 and 0.79, respectively, despite being sampled concomitantly. The IG-1, IG-2, and UP soils demonstrated mean air saturation levels above the aeration threshold at 0.62, 0.76 and 0.41, respectively. Overall, the criterion for aeration is likely to be fulfilled in well-drained fields during most growing seasons, as the growing seasons frequently are problematically dry (Caviezel et al., 2017). Nevertheless, aeration issues may be prevalent during wet growing seasons, which can occur because
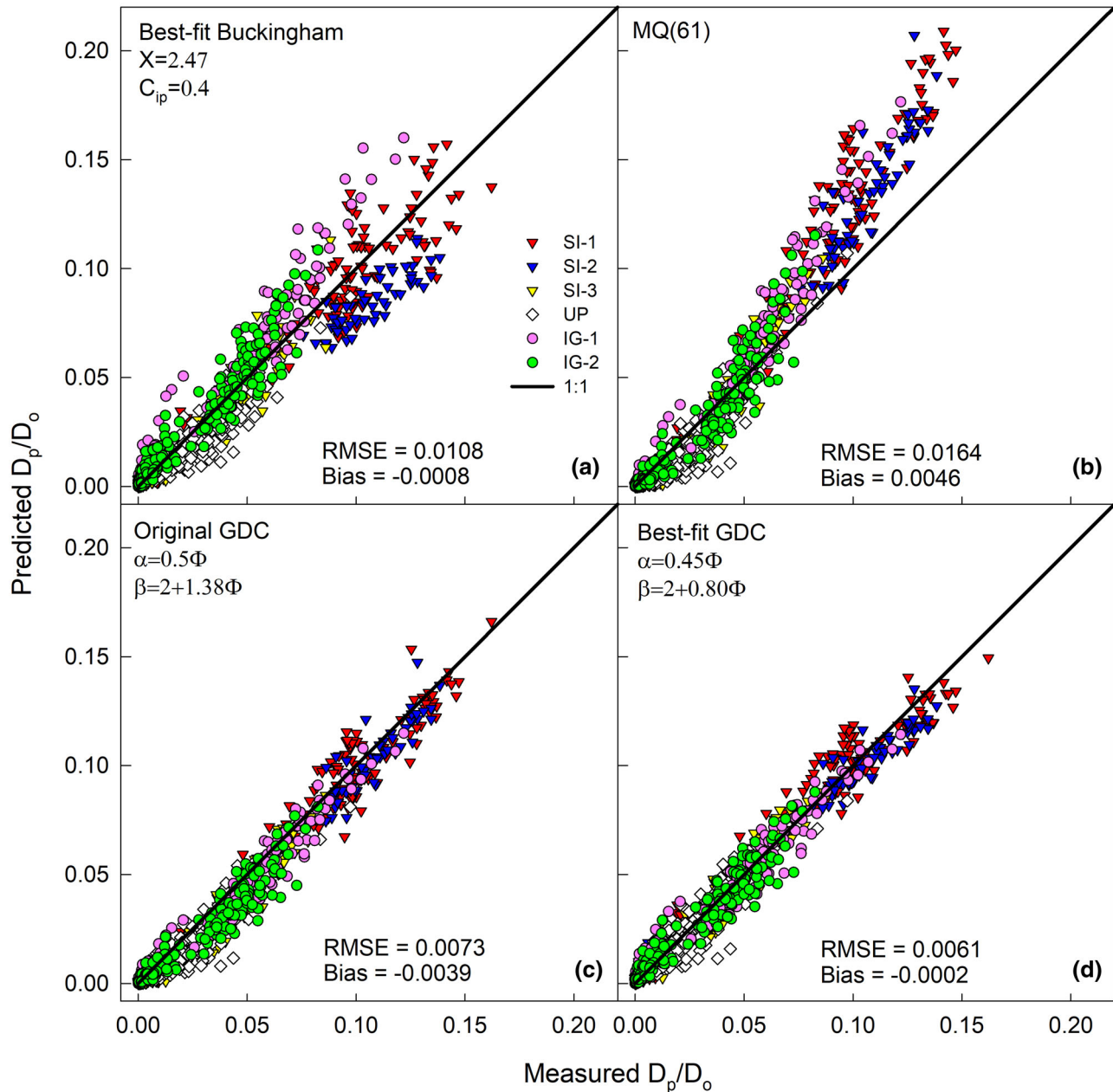
FIGURE 5 Scatterplot of predicted vs measured soil gas diffusivity [the soil gas diffusion coefficient (D_p)–free-air diffusion coefficient ratio, D_p/D_o] for four predictive models: (a) the best fitting Buckingham-type model (Equation 2), (b) the widely used Millington and Quirk (1961) model [MQ(61)] (Equation 4), (c) the original generalized density-corrected (GDC) model by Deepagoda et al. (2015) (Equation 5) with $\alpha = 0.5\Phi$ and $\beta = 2 + 1.38\Phi$, and (d) the best fitting GDC-type model (Equation 5) with $\alpha = 0.45\Phi$ and $\beta = 2 + 0.80\Phi$. Φ, total porosity.

of the high interannual variation in summer precipitation (Caviezel et al., 2017; Christensen et al., 2016).

A comparison of the predictive–descriptive ability across the tested models clearly highlighted the reduced variability of the models that included Φ (Figure 5). Consequently, the fitted GDC had almost double the descriptive power (RMSE = 0.0061) of the fitted Buckingham model (RMSE = 0.0108) (Figure 5a,d). The widely used MQ(61) model had the poorest predictive performance of all the tested models with an RMSE of 0.0164 (Figure 5b).

The MQ(61) model resulted in underpredictions in the wet region and overpredictions in the dry region, which is a general behavior of the model that has been reported on temperate soils (e.g. Deepagoda et al., 2011a; Deepagoda et al., 2012; Kawamoto et al., 2006). The original GDC model (Figure 5c) had remarkable prediction accuracy with an RMSE of 0.0073 but with small underpredictions at low to intermediate D_p/D_o values, resulting in a bias of −0.0039. A subsequent fitting of the GDC model resulted in the shape parameters $\alpha = 0.45\Phi$ and $\beta = 2 +$
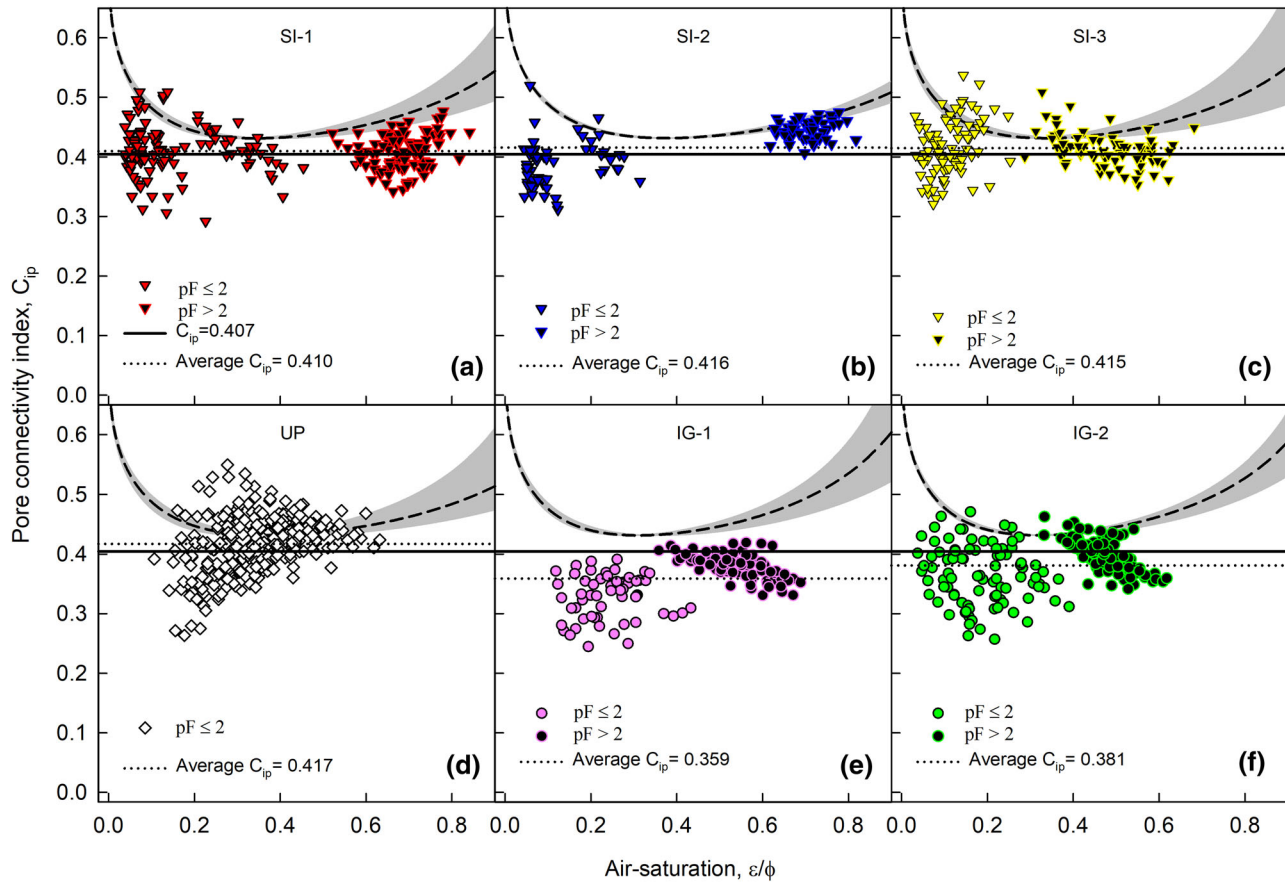
FIGURE 6 Variation of the pore connectivity index, (C_{ip}) (Equation 6), as a function of air saturation [the ratio of air-filled porosity (ε) to total porosity (Φ), ε/Φ] across the six fields: (a) South Igaliku Site 1, (b) South Igaliku Site 2, (c) South Igaliku Site 3, (d) Upernaviasuk, (e) Igaliku Site 1, and (f) Igaliku Site 2. Color-filled symbols denote measurements at pF ≤ 2, where pF = log[−ψ(cm H₂O)] and ψ is the soil water matric potential; black-filled symbols denote measurements at pF > 2. The lines represent the average C_{ip} across all fields (C_{ip} = 0.407, solid black lines) and the field-average C_{ip} (dotted black lines). The dashed line denotes the macroporosity-dependent (MPD) model (Moldrup et al., 2000) at field-average porosity; and the gray area represents the range between the minimum and maximum porosity

0.80Φ (Figure 5d), reflecting the slightly higher degree of pore network connectivity at low ε/Φ values than in the temperate soils the original GDC model was trained on.

3.4 | Structural fingerprints

The Greenlandic soils all displayed unique structural fingerprints in their C_{ip}–ε/Φ characteristic (Figure 6a–f). The C_{ip} derived from the MPD model, which was chosen to represent temperate Danish soils, resembles an upper boundary in C_{ip} for the SI and IG fields. (Figure 6). The Greenlandic soils generally displayed a lower and more constant C_{ip} across the measured range of ε/Φ, probably because of a less developed soil structure in combination with the high SOM content and high OC/clay ratio. A direct comparison of the Greenlandic C_{ip}–ε/Φ characteristics with the MPD model particularly highlighted the absence of pronounced

macroporosity, which would result in the marked increase in C_{ip} at low ε/Φ values as predicted by the MPD model (Deepagoda et al., 2015; Moldrup et al., 2000). Despite their high similarity, the two IG fields exhibited markedly different C_{ip}–ε/Φ characteristics (Figure 6e, f), which was probably a result of the IG-1 soil recently being tilled and thus having a less developed and more truncated macroporosity (Deepagoda et al., 2015; Fujikawa & Miyazaki, 2005). In contrast to SI-1, SI-2, and the IG fields, SI-3 displayed markedly higher C_{ip} values at intermediate ε/Φ values (Figure 6c). The UP field (Figure 6d) showed a highly variable C_{ip} within a narrow air saturation interval, which was probably caused by the higher content of gravel and stones (CF) either truncating the pore network or facilitating shrinkage-induced macropores at the CF–soil interface. In agreement with the latter idea, a small but significant ($P < .001$) positive linear correlation between C_{ip} and CF was found for UP at soil water potentials of pF1 and pF 1.5:
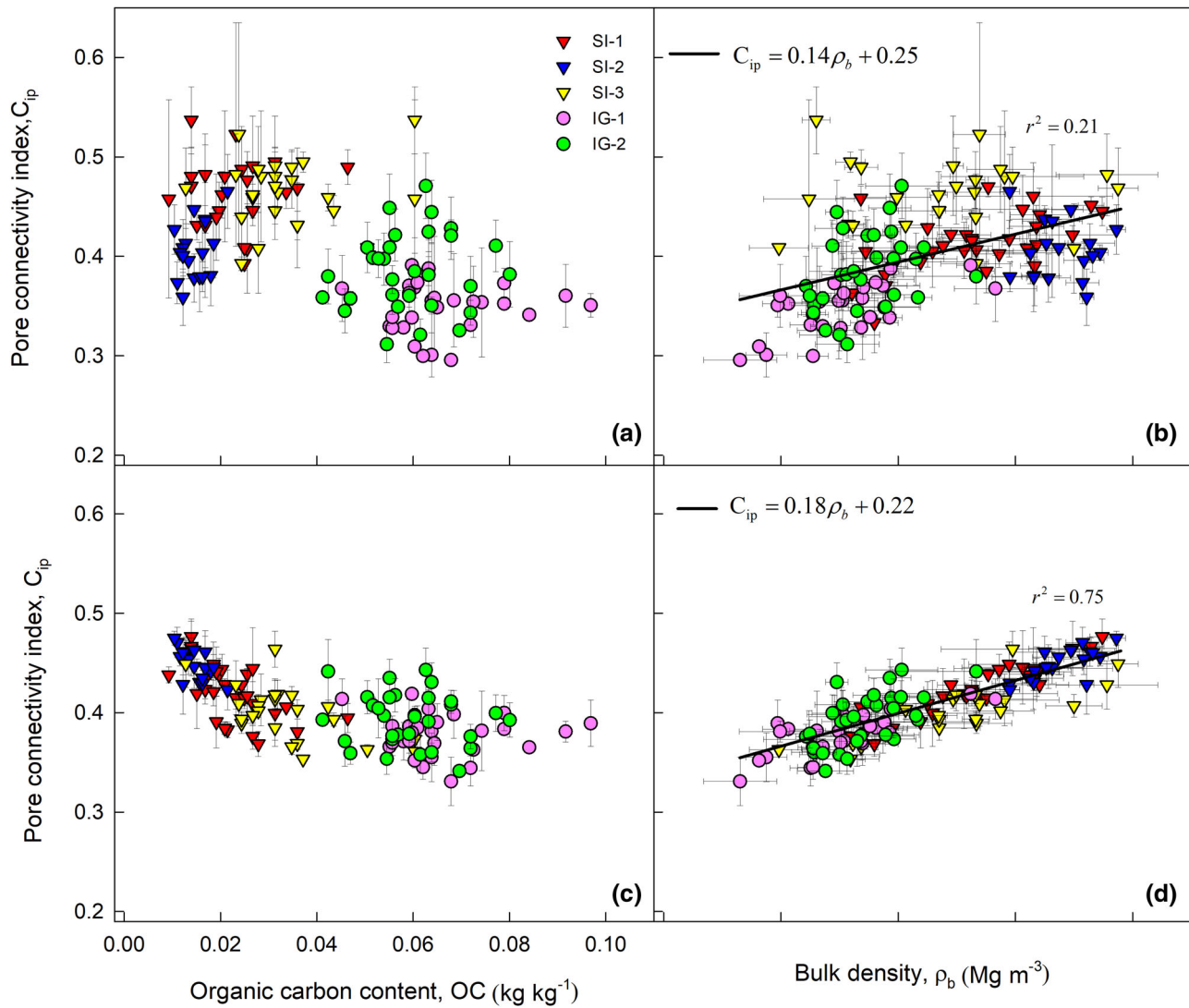
FIGURE 7 Pore connectivity index at pF2 (a, b) and pF3 (c, d) as a function of (a,c) organic C and (b, d) soil dry bulk density for five of the six investigated fields, where pF = log[−ψ (cm H$_2$O)] and ψ is the soil water matric potential. Error bars denote the SD. SI, South Igaliku; IG, Igaliku

$$C_{ip:pF1} = 1.05CF − 0.88; r^2 = 0.35 \quad (11)$$

$$C_{ip:pF1.5} = 1.20CF − 0.17; r^2 = 0.34, \quad (12)$$

where $C_{ip:pF1}$ and $C_{ip:pF1.5}$ are the C_{ip} at pF1 and pF1.5, respectively, and CF is the mineral CF in kg kg$^{−1}$.

The C_{ip} at both pF2 and pF3 decreased nonlinearly with OC and increased linearly with ρ$_b$ for the SI and IG soils (Figure 7). The pF2 state represents the typical field capacity for this texture range in a temperate climate (Al Majou, Bruand, & Duval, 2008; Nemes, Pachepsky, & Timlin, 2011), namely the amount of water retained in the soil a few days after a significant irrigation or drainage event (Romano & Santini, 2002). Furthermore, this water state would mimic climate change towards more temperate con-

ditions and/or higher irrigation of cultivated land in Southern Greenland. At pF2, the larger pores (>30 μm) were drained but there would still be water bridges blocking some interaggregate air pathways. The high C_{ip} of SI-3, therefore, indicates a more developed interaggregate pore space than in the other fields, which also would explain the high C_{ip} values at intermediate air saturation in Figure 6c The pF3 state will be closer to the current more arid conditions in Southern Greenland. In this state, the interaggregate pore space has typically drained fully (>3 μm) and therefore, the largest pore network connectivity and continuity in the soil–air phase will typically occur close to pF3 (Deepagoda et al., 2011b; Resurreccion et al., 2008). Since the soil–air phase at pF3 is less affected by water blockage, a more clear relationship between C_{ip} and ρ$_b$ was observed (Figure 7d). The strong positive linear correlation found

between ρ_b and C_{ip} at pF3 further showed ρ_b to be the principal physical parameter governing D_p/D_o in the Greenlandic soils; a subsequent multiple linear regression with clay and OC content did not produce a significant improvement ($P < .05$).

The overall findings of this study indicate a lack of well-developed structure in these highly porous Greenlandic agricultural soils, which negatively affected the diffusive gas fluxes throughout the measured range of soil water potentials. In particular, the lack of large and continuous macropore features may render these soils especially sensitive to hypoxia in poorly drained soils. Both the original and fitted GDC models provided good predictive–descriptive ability in the Greenlandic soils, which highlights the versatility of these density-corrected parametric models. Further testing is ultimately needed to validate the applicability of these density-corrected models on a wider range of Greenlandic, alpine, and (sub)Arctic agricultural soils. The present study covers a relatively narrow range in land use, OC, texture, and ρ_b, and further inquiry is needed to probe the gas diffusion characteristics of these northern agricultural soils.

4 | CONCLUSIONS

The soils exhibited higher Φ than temperate agricultural soils because of the low ρ_b and high ρ_s of the mineral and organic components.

The application of a density-corrected soil gas diffusivity model [i.e., including air saturation (ε/Φ) instead of ε as the main parameter] doubled the descriptive–predictive performance. However, model constants representing pore network tortuosity and connectivity differed from the original model, which was developed on temperate soils.

Moreover, the Greenlandic soils exhibited fundamental differences in pore network connectivity, as measured by C_{ip}, compared with temperate, long-term cultivated soils from Denmark. The C_{ip} was generally lower and more constant as a function of soil air saturation, which indicates a less developed soil structure together with the high OM and OC/clay ratios.

On the basis of the measured soil gas diffusivities and the best performing D_p/D_o model, air saturation above 35% is required to ensure adequate soil aeration ($D_p/D_o > 0.02$) for plant growth in the Greenlandic soils. This criterion for adequate aeration is expected to be fulfilled for well-drained soils during the growing season, as the present climatic conditions in South Greenland are relatively arid.

CONFLICT OF INTEREST
The authors declare that there is no conflict of interest.

ORCID
Peter L. Weber https://orcid.org/0000-0001-9249-0796

REFERENCES

Adderley, W. P., & Simpson, I. A. (2006). Soils and palaeo-climate based evidence for irrigation requirements in Norse Greenland. *Journal of Archaeological Science*, *33*(12), 1666–1679. https://doi.org/10.1016/j.jas.2006.02.014

Al Majou, H., Bruand, A., & Duval, O. (2008). The use of in situ volumetric water content at field capacity to improve the prediction of soil water retention properties. *Canadian Journal of Soil Science*, *88*(4), 533–541. https://doi.org/10.4141/CJSS07065

Ball, B. C. (1981). Modelling of soil pores as tubes using gas permeabilities, gas diffusivities and water release. *Journal of Soil Science*, *32*(4), 465–481. https://doi.org/10.1111/j.1365-2389.1981.tb01723.x

Ball, B. C. (2013). Soil structure and greenhouse gas emissions: A synthesis of 20 years of experimentation. *European Journal of Soil Science*, *64*(3), 357–373. https://doi.org/10.1111/ejss.12013

Bichet, V., Gauthier, E., Massa, C., Perren, B., Richard, H., Petit, C., & Mathieu, O. (2013). The history and impacts of farming activities in south Greenland: An insight from lake deposits. *Polar Record*, *49*(3), 210–220. https://doi.org/10.1017/S0032247412000587

Blake, G. R., & Hartge, K. H. (1986). Particle Density. In A. Klute (Eds.), *Methods of soil analysis: Part 1—Physical and mineralogical methods* (pp. 377–382). Madison, WI: Soil Science Society of America, American Society of Agronomy.

Buckingham, E. (1904). *Contributions to our knowledge of the aeration of soils*. Washington, DC: US Government Printing Office.

Caviezel, C., Hunziker, M., & Kuhn, N. (2017). Bequest of the Norseman—The potential for agricultural intensification and expansion in Southern Greenland under climate change. *Land*, *6*(4), 87. https://doi.org/10.3390/land6040087

Christensen, J. H., Olesen, M., Boberg, F., Stendel, M., & Koldtoft, I. (2016). *Fremtidige klimaforandringer i Grønland: Kujalleq Kommune*. Retrieved from https://www.dmi.dk/fileadmin/user_upload/Rapporter/SR/2015/15-04-01_kujalleq.pdf

Currie, J. A. (1960). Gaseous diffusion in porous media Part 1. – A non-steady state method. *British Journal of Applied Physics*, *11*(8), 314–317. https://doi.org/10.1088/0508-3443/11/8/302

Daanen, R. P., Ingeman-Nielsen, T., Marchenko, S. S., Romanovsky, V. E., Foged, N., Stendel, M., … Svendsen, K. H. (2011). Permafrost degradation risk zone assessment using simulation models. *The Cryosphere*, *5*(4), 1043–1056. https://doi.org/10.5194/tc-5-1043-2011

Deepagoda, T. K. K. C., Clough, T. J., Thomas, S. M., Balaine, N., & Elberling, B. (2019). Density effects on soil-water characteristics, soil-gas diffusivity, and emissions of N_2O and N_2 from a re-packed pasture soil. *Soil Science Society of America Journal*, *83*(1), 118–125. https://doi.org/10.2136/sssaj2018.01.0048

Deepagoda, T. K. K. C., de Jonge, L. W., Kawamoto, K., Komatsu, T., & Moldrup, P. (2015). The water-induced linear reduction gas

diffusivity model extended to three pore regions. *Vadose Zone Journal*, *14*(10), 1–9. https://doi.org/10.2136/vzj2015.04.0051

Deepagoda, T. K. K. C., Moldrup, P., Schjønning, P., Jonge, L. W. d., Kawamoto, K., & Komatsu, T. (2011a). Density-corrected models for gas diffusivity and air permeability in unsaturated soil. *Vadose Zone Journal*, *10*(1), 226–238. https://doi.org/10.2136/vzj2009.0137

Deepagoda, T. K. K. C., Moldrup, P., Schjønning, P., Kawamoto, K., Komatsu, T., & de Jonge, L. W. (2012). Variable pore connectivity model linking gas diffusivity and air-phase tortuosity to soil matric potential. *Vadose Zone Journal*, *11*(1). https://doi.org/10.2136/vzj2011.0096

Deepagoda, T. K. K. C., Moldrup, P., Schjønning, P., Kawamoto, K., Komatsu, T., & Wollesen de Jonge, L. (2011b). Generalized density-corrected model for gas diffusivity in variably saturated soils. *Soil Science Society of America Journal*, *75*(4), 1315–1329. https://doi.org/10.2136/sssaj2010.0405

Doran, J. W., & Parkin, T. B. (1994). Defining and assessing soil quality. In J. W. Doran, D. C. Coleman, D. F. Bezdicek, & B. A. Stewart (Eds.), *Defining soil quality for a sustainable environment* (pp. 1–21). Madison, WI: Soil Science Society of America and American Society of Agronomy.

Dugmore, A. J., Keller, C., & McGovern, T. H. (2007). Norse Greenland settlement: Reflections on climate change, trade, and the contrasting fates of human settlements in the North Atlantic islands. *Arctic Anthropology*, *44*(1), 12–36. https://doi.org/10.1353/arc.2011.0038

Francis, J. A., & Vavrus, S. J. (2012). Evidence linking Arctic amplification to extreme weather in mid-latitudes. *Geophysical Research Letters*, *39*(6), L06801. https://doi.org/10.1029/2012gl051000

Fujikawa, T., & Miyazaki, T. (2005). Effects of bulk density and soil type on the gas diffusion coefficient in repacked and undisturbed soils. *Soil Science*, *170*(11), 892–901. https://doi.org/10.1097/01.ss.0000196771.53574.79

Gee, G. W., & Or, D. (2002). Particle-size analysis. In J. H. Dane & C. G. Topp (Eds.), *Methods of soil analysis: Part 4—Physical methods* (pp. 255–293). Madison, WI: Soil Science Society of America.

Hanna, E., & Cappelen, J. (2002). Recent climate of southern Greenland. *Weather*, *57*(9), 320–328. https://doi.org/10.1256/00431650260283497

Hossain, M. F., Chen, W., & Zhang, Y. (2015). Bulk density of mineral and organic soils in the Canada's Arctic and sub-Arctic. *Information Processing in Agriculture*, *2*(3), 183–190. https://doi.org/10.1016/j.inpa.2015.09.001

Iiyama, I., & Hasegawa, S. (2005). Gas diffusion coefficient of undisturbed peat soils. *Soil Science and Plant Nutrition*, *51*(3), 431–435. https://doi.org/10.1111/j.1747-0765.2005.tb00049.x

Jacobsen, N. K. (1987). Studies on soils and potential for soil erosion in the sheep farming area of South Greenland. *Arctic and Alpine Research*, *19*(4), 498–507. https://doi.org/10.1080/00040851.1987.12002632

Jakobsen, B. H. (1991). Multiple processes in formation of subarctic podzols in Greenland. *Soil Science*, *152*(6), 414–426. https://doi.org/10.1097/00010694-199112000-00003

Jin, Y., & Jury, W. A. (1996). Characterizing the dependence of gas diffusion coefficient on soil properties. *Soil Science Society of America Journal*, *60*(1), 66–71. https://doi.org/10.2136/sssaj1996.03615995006000010012x

Kawamoto, K., Moldrup, P., Schjønning, P., Iversen, B. V., Rolston, D. E., & Komatsu, T. (2006). Gas transport parameters in the

vadose zone. *Vadose Zone Journal*, *5*(4), 1194–1204. https://doi.org/10.2136/vzj2006.0014

Marshall, T. J. (1959). The diffusion of gases through porous media. *Journal of Soil Science*, *10*(1), 79–82. https://doi.org/10.1111/j.1365-2389.1959.tb00667.x

Massa, C., Bichet, V., Gauthier, É., Perren, B. B., Mathieu, O., Petit, C., … Richard, H. (2012). A 2500 year record of natural and anthropogenic soil erosion in South Greenland. *Quaternary Science Reviews*, *32*, 119–130. https://doi.org/10.1016/j.quascirev.2011.11.014

Millington, R. J. (1959). Gas diffusion in porous media. *Science*, *130*(3367), 100–102. https://doi.org/10.1126/science.130.3367.100-a

Millington, R. J., & Quirk, J. M. (1960). Transport in porous media. In F. A. Van Beren, et al. (Eds.), *7th Transactions of the International Congress of Soil Science*, Vol. *1*, 14–24 Aug. 1960, Madison, WI (pp. 97–106). Amsterdam: Elsevier.

Millington, R. J., & Quirk, J. M. (1961). Permeability of porous solids. *Transactions of the Faraday Society*, *57*(0), 1200–1207. https://doi.org/10.1039/TF9615701200

Moldrup, P., Olesen, T., Komatsu, T., Schjønning, P., & Rolston, D. E. (2001). Tortuosity, diffusivity, and permeability in the soil liquid and gaseous phases. *Soil Science Society of America Journal*, *65*(3), 613–623. https://doi.org/10.2136/sssaj2001.653613x

Moldrup, P., Olesen, T., Schjønning, P., Yamaguchi, T., & Rolston, D. E. (2000). Predicting the gas diffusion coefficient in undisturbed soil from soil water characteristics. *Soil Science Society of America Journal*, *64*(1), 94–100. https://doi.org/10.2136/sssaj2000.64194x

Nemes, A., Pachepsky, Y. A., & Timlin, D. J. (2011). Toward improving global estimates of field soil water capacity. *Soil Science Society of America Journal*, *75*(3), 807–812. https://doi.org/10.2136/sssaj2010.0251

Nuttall, M. (2018). Arctic environments and peoples. In H. Callan (Ed.), *The International Encyclopedia of Anthropology* (pp. 1–7). Hoboken, NJ: John Wiley & Sons, Ltd.

Ogrič, M., Knadel, M., Kristiansen, S. M., Peng, Y., De Jonge, L. W., Adhikari, K., & Greve, M. H. (2019). Soil organic carbon predictions in Subarctic Greenland by visible–near infrared spectroscopy. *Arctic, Antarctic, and Alpine Research*, *51*(1), 490–505. https://doi.org/10.1080/15230430.2019.1679939

Penman, H. L. (1940). Gas and vapour movements in the soil: I. The diffusion of vapours through porous solids. *The Journal of Agricultural Science*, *30*(3), 437–462. https://doi.org/10.1017/S0021859600048164

Petersen, S. O., Schjønning, P., Thomsen, I. K., & Christensen, B. T. (2008). Nitrous oxide evolution from structurally intact soil as influenced by tillage and soil water content. *Soil Biology and Biochemistry*, *40*(4), 967–977. https://doi.org/10.1016/j.soilbio.2007.11.017

Pribyl, D. W. (2010). A critical review of the conventional SOC to SOM conversion factor. *Geoderma*, *156*(3), 75–83. https://doi.org/10.1016/j.geoderma.2010.02.003

Resurreccion, A. C., Moldrup, P., Kawamoto, K., Hamamoto, S., Rolston, D. E., & Komatsu, T. (2010). Hierarchical, bimodal model for gas diffusivity in aggregated, unsaturated soils. *Soil Science Society of America Journal*, *74*(2), 481–491. https://doi.org/10.2136/sssaj2009.0055

Resurreccion, A. C., Moldrup, P., Kawamoto, K., Yoshikawa, S., Rolston, D. E., & Komatsu, T. (2008). Variable pore connectivity factor

model for gas diffusivity in unsaturated, aggregated soil. *Vadose Zone Journal*, *7*(2), 397–405. https://doi.org/10.2136/vzj2007.0058

Rolston, D. E., & Moldrup, P. (2002). Gas – Diffusivity. In J. H. Dane & C. G. Topp (Eds.), *Methods of soil analysis: Part 4—Physical methods* (pp. 1113–1139). Madison, WI: Soil Science Society of America.

Romano, N., & Santini, A. (2002). Water retention and storage: field. In J. H. Dane & C. G. Topp (Eds.), *Methods of soil analysis: Part 4—Physical methods* (pp. 721–738). Madison, WI: Soil Science Society of America.

Ruehlmann, J., & Körschens, M. (2009). Calculating the effect of soil organic matter concentration on soil bulk density. *Soil Science Society of America Journal*, *73*(3), 876–885. https://doi.org/10.2136/sssaj2007.0149

Rühlmann, J., Körschens, M., & Graefe, J. (2006). A new approach to calculate the particle density of soils considering properties of the soil organic matter and the mineral matrix. *Geoderma*, *130*(3), 272–283. https://doi.org/10.1016/j.geoderma.2005.01.024

Rutherford, G. K. (1995). Soils of some Norse settlements in Southwestern Greenland. *Arctic*, *48*(4), 324–328. https://doi.org/10.14430/arctic1254

Schjønning, P., Eden, M., Moldrup, P., & de Jonge, L. W. (2013a). Two-chamber, two-gas and one-chamber, one-gas methods for measuring the soil-gas diffusion coefficient: Validation and intercalibration. *Soil Science Society of America Journal*, *77*(3), 729–740. https://doi.org/10.2136/sssaj2012.0379

Schjønning, P., Lamandé, M., Berisso, F. E., Simojoki, A., Alakukku, L., & Andreasen, R. R. (2013b). Gas diffusion, non-Darcy air permeability, and computed tomography images of a clay subsoil affected by compaction. *Soil Science Society of America Journal*, *77*(6), 1977–1990. https://doi.org/10.2136/sssaj2013.06.0224

Schjønning, P., McBride, R. A., Keller, T., & Obour, P. B. (2017). Predicting soil particle density from clay and soil organic matter contents. *Geoderma*, *286*, 83–87. https://doi.org/10.1016/j.geoderma.2016.10.020

Schjønning, P., Thomsen, I. K., Moldrup, P., & Christensen, B. T. (2003). Linking soil microbial activity to water- and air-phase contents and diffusivities. *Soil Science Society of America Journal*, *67*(1), 156–165. https://doi.org/10.2136/sssaj2003.1560

Schofield, J. E., Edwards, K. J., Mighall, T. M., Martínez Cortizas, A., Rodríguez-Racedo, J., & Cook, G. (2010). An integrated geochemical and palynological study of human impacts, soil erosion and storminess from southern Greenland since c. AD 1000. *Palaeogeography, Palaeoclimatology, Palaeoecology*, *295*(1), 19–30. https://doi.org/10.1016/j.palaeo.2010.05.011

Schofield, R. K. (1935). The pF of the water in soil. In *Transactions of the Third International Congress on Soil Science*, Vol. *2*, July–August 1935, Oxford, UK. (pp. 37–48). Oxford, UK: Murby & Co.

Schulze, E. D., Luyssaert, S., Ciais, P., Freibauer, A., Janssens, I. A., Soussana, J. F., … Heimann, M. (2009). Importance of methane and nitrous oxide for Europe's terrestrial greenhouse-gas balance. *Nature Geoscience*, *2*(12), 842–850. https://doi.org/10.1038/ngeo686

Smith, K. A., Dobbie, K. E., Ball, B. C., Bakken, L. R., Sitaula, B. K., Hansen, S., … Orlanski, P. (2000). Oxidation of atmospheric methane in Northern European soils, comparison with other ecosystems, and uncertainties in the global terrestrial sink. *Global Change Biology*, *6*(7), 791–803. https://doi.org/10.1046/j.1365-2486.2000.00356.x

Stepniewski, W. (1980). Oxygen-diffusion and strength as related to soil compaction. I. ODR. *Polish Journal of Soil Science*, *13*(1), 3–13.

Stepniewski, W. (1981). Oxygen diffusion and strength as related to soil compaction. II. Oxygen diffusion coefficient. *Polish Journal of Soil Science*, *14*, 3–13.

Tang, J., & Riley, W. J. (2019). A theory of effective microbial substrate affinity parameters in variably saturated soils and an example application to aerobic soil heterotrophic respiration. *Journal of Geophysical Research: Biogeosciences*, *124*(4), 918–940. https://doi.org/10.1029/2018jg004779

Westergaard-Nielsen, A., Bjørnsson, A. B., Jepsen, M. R., Stendel, M., Hansen, B. U., & Elberling, B. (2015). Greenlandic sheep farming controlled by vegetation response today and at the end of the 21st century. *Science of The Total Environment*, *512–513*, 672–681. https://doi.org/10.1016/j.scitotenv.2015.01.039